

Orientational Melting and Reorientational Motion in a Cubane Molecular Crystal: A Molecular Simulation Study

N. Arul Murugan

Solid State and Structural Chemistry Unit, Indian Institute of Science, Bangalore-560012, India

Received: May 13, 2005; In Final Form: October 30, 2005

Detailed molecular simulations are carried out to investigate the effect of temperature on orientational order in cubane molecular crystal. We report a transition from an orientationally ordered to an orientationally disordered plastic crystalline phase in the temperature range 425–450 K. This is similar to the experimentally reported transition at 395 K. The nature of this transition is first order and is associated with a 4.8% increase in unit cell volume that is comparable to the experimentally reported unit cell volume change of 5.4% (*Phys. Rev. Lett.* **1997**, 78, 4938). An orientational order parameter, $\eta(T)$, has been defined in terms of average angle of libration of a molecular 3-fold axis and the orientational melting has been characterized by using $\eta(T)$. The orientational melting is associated with an anomaly in specific heat at constant pressure (C_p) and compressibility (κ). The enthalpy of transition and entropy of transition associated with this orientational melting are 20.8 J mol⁻¹ and 0.046 J mol⁻¹ K⁻¹, respectively. The structure of crystalline as well as plastic crystalline phases is characterized by using various radial distribution functions and orientational distribution functions. The coefficient of thermal expansion of the plastic crystalline phase is more than twice that of the crystalline phase.

1. Introduction

Organic molecular crystals show different types of disorder^{1,2} associated with conformational,³ orientational,⁴ vibrational,⁵ and in-plane-reorientational⁶ degrees of freedom of molecules. The type of disorder in a molecular crystal is largely decided by the geometry of the individual molecule. Crystals of globular shape molecules⁴ such as adamantane,⁷ its derivatives,⁸ and C₆₀, molecules with tetrahedral structure such as methane and its halo derivatives,⁹ and molecules with octahedral structure like SF₆⁹ transform to an orientationally disordered phase at higher temperatures. The orientationally disordered plastic crystalline phases are characterized by a low entropy of fusion that is usually less than 20 J K⁻¹ mol⁻¹.^{4,10} Interestingly, a cubane crystal with cubelike molecular structure has also been reported to show a transition to an orientationally disordered phase at 394 K.^{11–14} In this paper, the structure of orientationally ordered and disordered phases of cubane molecular crystal and the nature of the transition are investigated in detail.

After the synthesis of cubane by Eaton and Cole in 1964,¹⁵ there are many experimental as well as theoretical studies^{11–24} on the cubane molecule and its condensed phase. Cubane is a highly strained molecule and is a promising candidate for use as a high-energy material and fuel. In its condensed phase, cubane has a relatively larger density and heat of formation²⁵ than other cage-like hydrocarbons. High strain in the molecular structure shifts the C–C stretching frequencies to higher values ranging from 822 to 1024 cm⁻¹. But C–H stretching frequencies are observed approximately at 3000 cm⁻¹ similar to those in unstrained hydrocarbons.¹⁶

X-ray diffraction investigations showed that cubane crystallizes in a rhombohedral structure with cell parameters $a = 5.34$ Å, $\alpha = 72.7^\circ$, and $Z = 1$.¹⁷ Temperature-dependent X-ray diffraction results reveal that the high-temperature orientationally disordered phase is surprisingly not cubic and instead it is

rhombohedral with $\alpha = 103.3^\circ$.^{18,19} This is unlike most plastic crystalline phases which are frequently cubic. The transition of orientationally ordered phase to an orientationally disordered phase is first order and is associated with a unit cell volume change of 5.4%.¹⁸ The lattice exhibits high thermal expansion probably due to large-amplitude rotations of cubane molecules. Yildirim et al.²⁰ studied orientational dynamics of the cubane molecules in solid phases above and below the orientational order–disorder transition temperature using neutron scattering techniques. In the orientationally ordered phase, the elastic incoherent structure factor (EISF) calculated from neutron time-of-flight measurements indicates that molecules undergo π jumps about the molecular 4-fold axis.²⁰ In the orientationally disordered phase, calculated EISF shows that the molecules undergo uncorrelated π jumps about the molecular 4-fold axis and $2\pi/3$ jumps about the 3-fold axis.²⁰

Richardson et al.²¹ studied the structure as well as electronic properties of solid cubane using the ab initio constant pressure extended molecular dynamics method with variable cell shape.²² These calculations could predict the experimentally observed¹⁷ distortion in C–C and C–H bond lengths reasonably well but the calculated lattice constants showed larger deviation from experimental results. The first principle calculations by Yildirim et al.¹⁶ using both Gaussian basis and plane wave basis could reproduce all peaks of the experimental neutron inelastic spectrum (NIS)²³ at correct energies with correct intensities.

Structure–energy relationships for solid cubane have been given as a function of rhombohedral cell parameter (a), angle (α), and setting angle (ϕ), using both first principle¹⁶ and lattice dynamics calculations.²⁴ The global and local minima observed in the derived relationships correspond to experimentally observed orientationally ordered and orientationally disordered crystalline phases, respectively. Even though there are many experimental and theoretical investigations on the cubane molecular crystal, the temperature dependence of reorientational

TABLE 1: Potential Parameters for Cubane

type	A, kJ/mol Å ⁶	B, kJ/mol	C, Å ⁻¹
C–C	1550.13	165809.15	3.60
C–H	543.21	30265.15	3.67
H–H	190.37	6355.20	3.74

motion of molecules, the nature of orientational disorder, and the coupling of orientational degrees of freedom of molecules with the degrees of freedom of the unit cell are not understood clearly. Insight into the reorientational motion of molecules and coupling of orientational disorder with unit cell parameters requires a detailed molecular simulation investigation on the cubane molecular crystal as a function of temperature. Here, we have studied solid cubane as a function of temperature using isothermal–isobaric Monte Carlo calculations with variable shape simulation cell. The effect of temperature on orientational order and reorientational motion of molecules has been studied. Structures of the orientationally ordered and disordered phases of the cubane molecular crystal have been characterized by various radial distribution functions (rdfs) and orientational distribution functions (odfs). Also, we discuss thermal expansion in crystalline and plastic crystalline phases based on the calculated coefficient of thermal expansion for these two phases.

2. Methods

2.1. Intermolecular Potential. A semiempirical atom–atom potential²⁶ of Buckingham 6-exp type with charge (see eq 1) has been employed to model the intermolecular interaction between cubane molecules.

$$u_{ij} = -A_{ij}/r_{ij}^6 + B_{ij}\exp(-r_{ij}C_{ij}) + q_iq_j/r_{ij} \quad (1)$$

Here i and j refer to atomic indices of different molecules.

The physical significance of the three terms in the potential model is as below: (i) First term ($-A_{ij}/r_{ij}^6$) is a long-range attractive dispersion energy, (ii) the second term ($B_{ij}\exp(-r_{ij}C_{ij})$) is a short-range repulsive energy due to overlapping of electron clouds, and (iii) the third term (q_iq_j/r_{ij}) is a very long-range Coulombic energy that can be either attractive or repulsive depending on the sign of the charge on sites i and j . For the nonpolar molecules, the relative importance of these three energies goes in the aforementioned order.

As the molecular electrostatic potential is important in reproducing correct crystal structure,²⁷ we have used a potential model with a Coulombic term. In the present case, the potential model places -0.1 e charge on carbon and 0.1 e charge on hydrogen atoms. The potential parameters A_{ij} , B_{ij} , and C_{ij} used to model intermolecular interaction in cubane molecular crystal are listed in Table 1. The lattice dynamics calculations by Yildirim²⁴ using these potential parameters²⁶ could reproduce the density of states obtained from inelastic neutron scattering measurements.²⁸ For the low-temperature phase at 100 K, the calculations could reproduce the distinct peaks at 78, 94, and 114 cm⁻¹ in the vibrational density of states.²⁸ Also, softening of these peaks for the high-temperature phase at 300 K²⁸ has also been reproduced. Moreover, the calculated libron and phonon energies were in good agreement with experimental data.²⁸ So, these potential parameters are used in our calculations without any modification.

2.2. Variable Shape Monte Carlo Simulations. Simulations have been carried out in an isothermal–isobaric or NPT ensemble with a variable shape simulation cell²⁹ with use of the Monte Carlo method and the importance sampling algorithm of Metropolis.³⁰ Many orientational and conformational order–

disorder phase transitions^{31,32} and structural phase transitions were successfully investigated with this method.^{33,34} In this method, the simulation cell is represented by six degrees of freedom after the subsequent modification by Yashonath and Rao³⁵ while original formulation by Parrinello and Rahman²⁹ used nine degrees of freedom to represent the simulation cell. Each molecule has a total of 6 degrees of freedom including 3 for translational and 3 for rotational motion and the average of any property a is obtained by integrating over these $(6N + 6)$ variables as in eq 2,

$$\langle a \rangle = \frac{\int da \int db \int dc \int d\Omega^N \int d\mathbf{r}^N a(\mathbf{r}^N, \Omega^N) p(\mathbf{r}^N, \Omega^N)}{\int da \int db \int dc \int d\Omega^N \int d\mathbf{r}^N p(\mathbf{r}^N, \Omega^N)} \quad (2)$$

where N is the number of molecules. $p(\mathbf{r}^N, \Omega^N) = e^{-\beta U(\mathbf{r}^N, \Omega^N)}$ and $a(\mathbf{r}^N, \Omega^N)$ are the probability and the property respectively for each configuration specified by (\mathbf{r}^N, Ω^N) . Here \mathbf{r}^N are the center of mass positions of the N molecules and Ω^N specify the orientations of the N molecular species. Note that \mathbf{r} and Ω have three components each: \mathbf{r} specifies the three Cartesian coordinates and Ω the three Euler angles.

2.3. Computational Details. The simulation box contains $7 \times 7 \times 7$ unit cells and a total of 343 molecules. Calculations were carried out at temperatures 295, 300, 325, 350, 375, 400, 425, 437.5, 450, 462.5, 475, 500, 525, and 550 K and at 1 atm of pressure. These calculations attempt to study temperature induced orientational order–disorder transition in the cubane molecular crystal. For the simulation at 295 K, the initial configuration was taken from the crystallographic structure provided by Fleischer.¹⁷ For the simulations other than at temperature 295 K, the initial configuration was taken from the previous low-temperature simulation. Each Monte Carlo move of a molecule involves a random displacement of center of mass (c.o.m.) and a random rotation of the molecule along a randomly selected axis. Each Monte Carlo move associated with the simulation cell involves a random displacement of all the cell parameters by a small value. Each Monte Carlo step involves the Monte Carlo move of all N molecules once and the Monte Carlo move of the simulation box once. The displacement maxima in Monte Carlo moves are adjusted so that the acceptance ratio is around 0.40. Each run involves 24 000 Monte Carlo (MC) steps including 4 000 MC steps for equilibration. The calculation of various structural quantities such as rdfs, odfs, average cell parameters, volume, and interaction energies involves averaging over 20 000 MC steps after equilibration. The c.o.m.–c.o.m. cutoff (r_c) of 13 Å has been used for the calculation of interaction energies. This cutoff has been used, as any further increase in r_c does not change the interaction energy significantly.

3. Results and Discussions

3.1. Structure and Energetics. Figure 1 shows the variation of various average structural parameters and average interaction energy as a function of temperature. Figure 1a shows the variation of cell parameters a , b , and c , Figure 1b shows the variation of unit cell volume, and Figure 1c shows the variation of total interaction energy as a function of temperature. Here, total interaction energy is given as

$$U_{\text{inter}} = \frac{1}{2N} \sum_{i=1}^{N_{\text{neigh}}} \sum_{j=1}^N u_{ij} \quad (3)$$

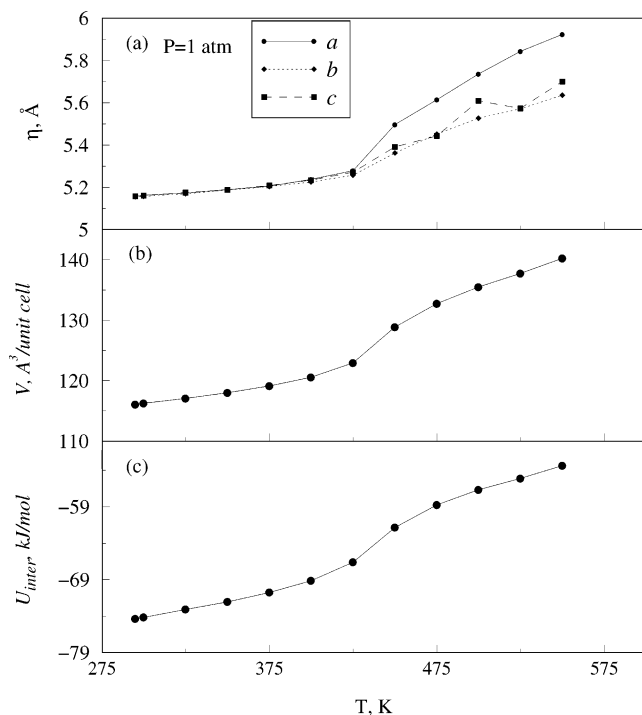


Figure 1. Variation of (a) cell parameters a , b , and c , (b) unit cell volume, and (c) total interaction energy as a function of temperature at 1 atm of pressure.

where N stands for the total number of molecules and $N_{j,\text{neigh}}$ stands for the number of molecules with the cutoff radius 13.0 Å around the molecule j . Here, j runs over all molecules and i runs over all molecules until the fourth shell of neighbors around the molecule j .

Compared to experimental results at room temperature, the cell parameters are reproduced well within the threshold limit of 3% allowed for cell edge shift.²⁷ At this temperature, the simulated cell parameters are $a = 5.2$ Å and $\alpha = 70^\circ$ while the experimental cell parameters are $a = 5.3$ Å and $\alpha = 72^\circ$. These results seem to be far better when compared with 9% deviation of cell parameters reported from ab initio electronic structure calculation with the plane wave basis.²¹

There is a discontinuity between 425 and 450 K in the temperature dependence of cell parameters, unit cell volume, and interaction energy. Later in this paper, it will be shown that this discontinuity is associated with the orientational order–disorder transition that has been reported experimentally at 395 K. The difference in transition temperature may be due to a slightly stronger interaction between the cubane molecules as predicted by the potential model. This transition is a first order transition that is consistent with experimental observation. This transition is associated with a 4.8% increase in unit cell volume, which can be compared with the experimentally reported unit cell volume change of 5.4%.¹⁸ Later in this paper, we will establish that the phase corresponding to the region above the transition temperature (between 425 and 450 K) is a plastic crystalline phase. It is evident from the plot of temperature dependence of unit cell volume that thermal expansion of the plastic crystalline phase is larger than that of the crystalline phase. We have calculated (see eq 4) the coefficient of thermal expansion (α) from the slopes $(\partial V/\partial T)$ of the two regions, i.e., above and below the transition. We have found that plastic crystalline phase has α 2.8 times greater than that of the crystalline phase. Table 2 lists the slopes from the linear fit to the two regions corresponding to crystalline and plastic crystal-

TABLE 2: Linear Fitting Data for the Two Regions in the Unit Cell Volume Variation as a Function of Temperature along with the Coefficient of Thermal Expansion for Orientationally Ordered and Disordered Phases

phase	slope $((\partial V/\partial T)_P)$, Å ³ K ⁻¹	constant, Å ³	α , 10 ⁻⁶ K ⁻¹
crystalline	0.050	101.1	490.9
plastic crystalline	0.111	79.6	1394.1

line phases in the plot of temperature dependence of unit cell volume.

$$\alpha = \frac{1}{V} \left(\frac{\partial V}{\partial T} \right)_P \quad (4)$$

The larger coefficient of thermal expansion of the plastic crystalline phase can be understood easily from large-amplitude reorientational motion of molecules in the plastic crystalline phase weakening the interactions between the molecules and hence allowing an easier thermal expansion.

Interestingly, present calculations show that the plastic crystal phase is stable for more than 75 K after the transition temperature, which is between 425 and 450 K. But experimentally, the plastic crystalline phase of cubane is stable only for 20 K after the transition temperature, 394 K.¹⁸ This is again due to the stronger interaction between the molecules predicted by the potential model and to super heating effect.^{36,37} The super heating effect has its origin in the fact that the rate of change in temperature or pressure in simulations is many times larger than that available to experimental techniques. Recent experimental investigations by Jin et al.³⁶ and Lu and Li³⁷ showed that by super heating a crystal, the crystal can be heated above its melting point.^{36,37} So, it is not very uncommon to observe higher melting temperatures or order–disorder transition temperatures in simulated molecular crystals when compared to experiments. There are many recent theoretical investigations which report much higher melting points for the crystals of nitromethane,³⁸ ammonium dinitramide,³⁹ and poly(tetrafluoroethylene)⁴⁰ and the higher melting point has been attributed to the super heating effect.^{36,37} Earlier, from our calculations we have also reported a higher transition temperature for orientational order–disorder transition in the case of adamantane.⁴¹ Moreover, in the case of stilbene⁴² we have reported that the conformational disorder seems to appear at slightly higher temperature compared to the experimentally reported transition temperature. With this understanding, it is not very surprising to see a higher melting point for the cubane molecular crystal. So, the plastic crystalline phase seems to be stable for a larger temperature range. The transition from the orientationally ordered phase to an orientationally disordered phase is associated with the 7.70% decrease in the magnitude of the interaction energy. Significant increase in unit cell volume at the transition temperature increases the interatomic distances and hence decreases the interaction energy.

Figure 2 shows the variation of dispersion energy, repulsion energy, and Coulombic energy as a function of temperature. Interestingly, variation of these quantities is associated with a discontinuity in the temperature range, 425–450 K. This is consistent with the temperature dependence of other structural quantities such as cell parameters, unit cell volume, and total interaction energy. With an increase in temperature the intermolecular distance increases (i.e., interatomic or site–site distance increases) as the unit cell volume increases. This results in a decrease in the dispersion energy as well as a decrease in the repulsion energy. Another observation is that above the

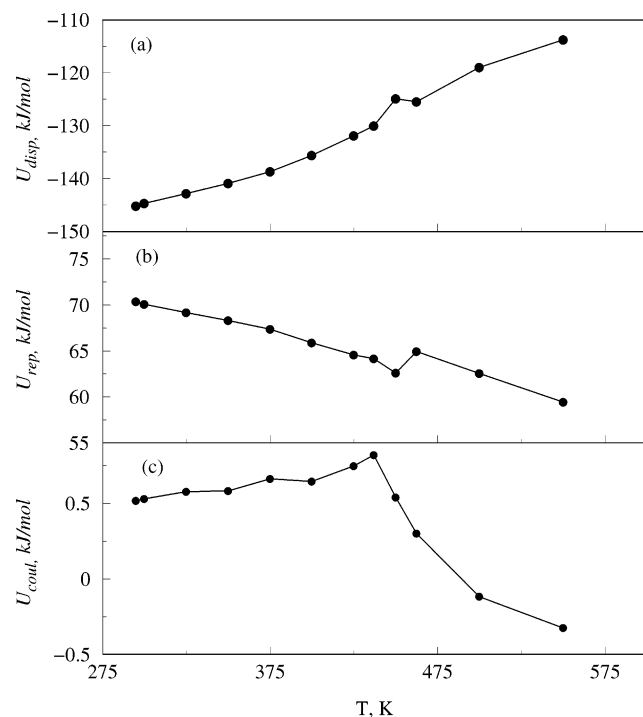


Figure 2. Variation of (a) dispersion energy, (b) repulsion energy, and (c) Coulombic energy as a function of temperature.

transition temperature, the Coulombic energy becomes increasingly negative. This can be understood as below: In the low temperature phase, the structure is such that like atoms (particularly H–H pairs) are closer. But with an increase in temperature, the structure becomes orientationally disordered resulting in the unlike atoms coming closer, bringing the negative contribution from Coulombic energy. It is to be noted that the contribution from Coulombic energy to the total interaction energy is less than 1%. But, still it is necessary to include the Coulombic term in the potential model to predict the crystal structure more accurately.²⁷

Figure 3 shows c.o.m.–c.o.m., C–C, C–H, and H–H rdfs as a function of temperature. It is evident from the figure that the rdfs display considerable changes at 450 K indicating a larger structural change at this temperature. Disappearance of sharp peaks in all atom–atom rdfs is an indication of onset of orientational disorder at 450 K. This type of evolution of atom–atom rdfs as a function of temperature has been observed in molecular crystals such as adamantane⁴¹ exhibiting orientational disorder and in crystals with conformational disorder such as stilbene⁴² and 4-vinylbenzoic acid.⁴³ In the present case, we attribute the partial melting of orientational degrees of freedom to the disappearance of sharp peaks and the appearance of liquidlike features in various atom–atom rdfs. In the c.o.m.–c.o.m. rdf at 450 K, the narrower peaks merge together resulting in broader peaks and this is an indication of significantly large amplitude translational motion. Near the orientational order–disorder transition, considerable increase in the translational disorder has been reported in other plastic crystalline systems such as neopentane.⁴⁴ When the molecules reorient from one most possible orientation to another, the neighboring molecules are pushed away and this results in an increase in the translational disorder. This is clearly seen in the temperature dependence of c.o.m.–c.o.m. rdf.

3.2. Reorientational Motion. To study the reorientational motion of cubane molecules, the three-dimensional orientational distribution function $f(\theta, \phi)$ of the vector \bar{n} has been computed. The vector \bar{n} is one of the 4-fold axes as shown in Figure 4. $f(\theta, \phi)$ is defined as

$$f(\theta, \phi) = \frac{1}{NN_{\text{step}}} \sum_{i=1}^N \sum_{j=1}^{N_{\text{step}}} [\delta(\theta - \theta_i)] [\delta(\phi - \phi_i)] \quad (5)$$

where N and N_{step} are the number of molecules and total number of MC steps, respectively. θ is the angle between the vector \bar{n} and x axis in the laboratory frame while ϕ is the angle between the vector \bar{n} and y axis in the laboratory frame (see Figure 4). θ_i and ϕ_i are the angles corresponding to i th molecule.

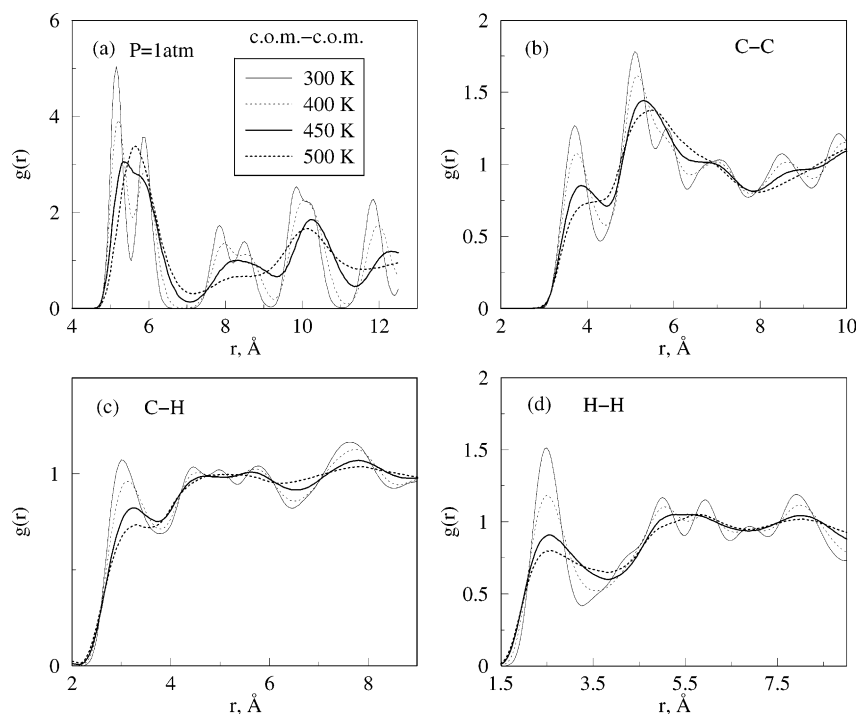


Figure 3. Various radial distribution functions at 300, 400, 450, and 500 K: (a) c.o.m.–c.o.m., (b) C–C, (c) C–H, and (d) H–H.

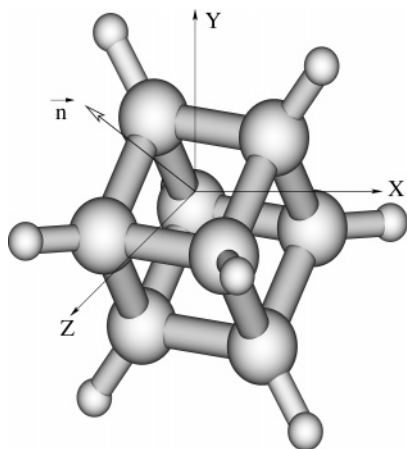


Figure 4. Molecular structure of cubane with a molecular 4-fold axis shown.

Figure 5 shows the contour plots of the orientational distribution function (odf) in the temperature range 300–550 K. At low temperatures up to 350 K, the distribution function displays only one preferential orientation. The angles θ and ϕ are distributed in the range between 90° and 110° . This clearly shows a small amplitude librational motion of molecules at this temperature. Between the temperatures 400 and 450 K, odf displays a larger change and more than one preferable orientation appears. This is an indication for the onset of orientational disorder. But still one can see a considerably large population of molecules in their initial starting orientations. We have already shown that the onset of orientational disorder is associated with a larger change in cell parameters, volume, and total interaction energy (see Figure 1). At 450 K, the distribution function displays five preferential orientations. Naturally cubane molecules will have six orientations in the space. When the orientations are projected over any of the planes (xy , yz , xz), we can have only five (as we see in the Figure 5). In Figure 5, we have plotted the orien-

tations projected in the xy plane. Initial orientations as well as the orientations after 180° or -180° flips of molecular 4-fold axis along the x or y axis in the laboratory frame will yield a single orientation (which is at $\theta = 90^\circ$, $\phi = 90^\circ$ in all the subplots of Figure 5). 90° or -90° flips of molecular 4-fold axis along the x axis will result in two more orientations at the points $\theta = 0^\circ$, $\phi = 90^\circ$ and $\theta = 180^\circ$, $\phi = 90^\circ$ in subplots d, e, and f of Figure 5. Similarly, 90° or -90° flips of molecular 4-fold axis along the y axis will result in two more orientations at the points $\theta = 90^\circ$, $\phi = 0^\circ$ and $\theta = 90^\circ$, $\phi = 180^\circ$ in the subplots d, e, and f of Figure 5. At 450 K, it is clearly seen that some orientations are forbidden because these orientations are energetically unfavorable. At 500 K, the domain of forbidden orientations reduces in size. At 550 K, almost all orientations become accessible for the molecules showing a complete orientational disorder at this temperature. It is important to note that the nature of evolution of odfs as a function of temperature remains the same independent of the pair of axes considered in the calculation of odfs. A detailed analysis of the calculated elastic incoherent structure factor and comparison to different rotational models is in progress that may shed more light on the rotational dynamics of molecules in the cubane molecular crystal at different temperatures.

In the low-temperature orientationally disordered crystalline phase of cubane, the molecular 3-fold axes are parallel to the crystallographic $[111]$ directions. So, the orientational disorder can be studied in terms of deviation of a molecular 3-fold axis relative to the crystallographic $[111]$ direction. We define ψ as an angle between a 3-fold axis and the crystallographic $[111]$ direction, which is parallel to this molecular axis. The distribution of this angle, $f(\psi)$, is given in eq 6. The calculation of $f(\psi)$ includes ψ calculated for all molecules over all MC steps

$$f(\psi) = \frac{1}{NN_{\text{step}}} \sum_{\text{step}}^N \sum_{i=1}^{N_{\text{step}}} \delta(\psi - \psi_i) \quad (6)$$

where ψ_i the angle corresponding to the i th molecule.

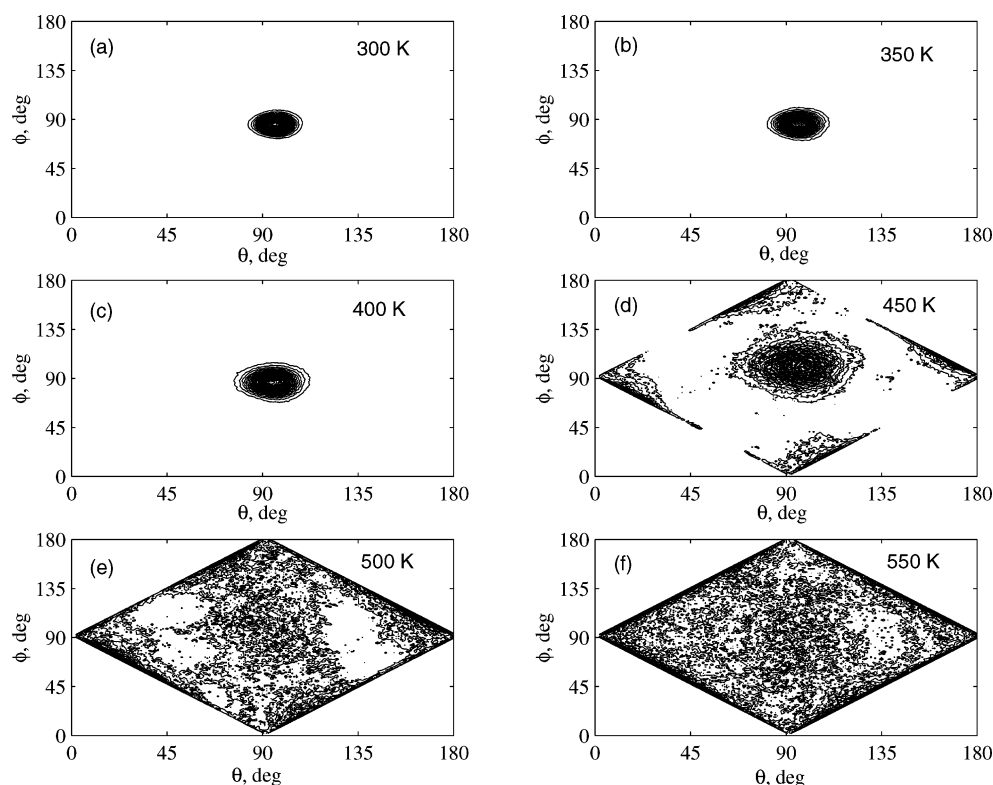


Figure 5. Orientational distribution function, $f(\theta, \phi)$, at different temperatures.

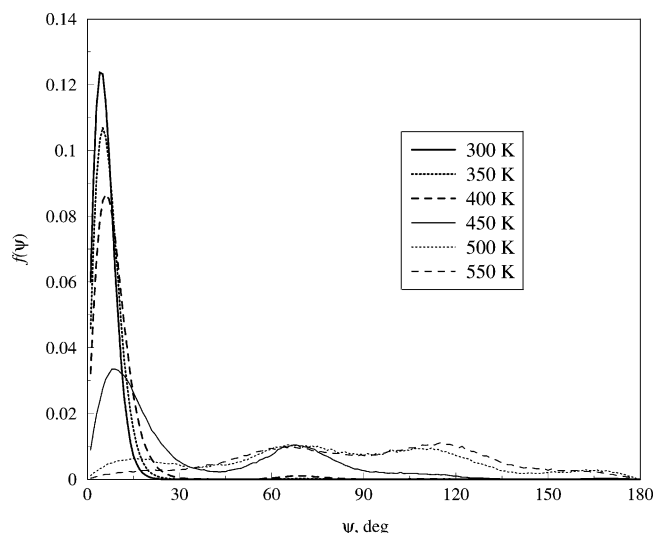


Figure 6. Orientational distribution function, $f(\psi)$, at different temperatures.

Figure 6 displays the orientational distribution function, $f(\psi)$. A single peak in the distribution function up to a temperature of 400 K clearly shows that molecules have restricted small amplitude reorientational motion. The peak appears closer to zero due to the fact that the molecular 3-fold axis is parallel to the crystallographic [111] direction. Up to this temperature, the distribution function spans a small angle range of 0–30°. At 450 K, the distribution function displays a considerable change and it covers the angle range between 0 and 135°. This clearly shows the onset of orientational disorder and a large amplitude motion of molecules at this temperature. It is to be noted that at this temperature, not all the orientations are equally probable. The neighboring molecular environment of the molecules makes some orientations preferable over other orientations. Beyond 450 K, the distribution function covers the entire angle range between 0 and 180° showing a complete orientational disorder within the system. In this temperature range, the peak-like features disappear in the distribution function. This is an indication of free rotation of molecules in a flat potential energy surface. This is in complete agreement with earlier investigations by Yildirim et al.^{18,24} which also showed the flattening of potential energy profile at higher temperatures.

Figure 7 shows the temperature dependence of the average angle of libration, $\langle\psi\rangle$. This has been obtained from eq 7.

$$\langle\psi\rangle = \sum_{j=0}^{180} \psi_j f(\psi_j) \quad (7)$$

It should be noted that the function $f(\psi)$ is normalized. The summation is over all the angles between 0 and 180°. $\langle\psi\rangle$ shows the nature of the reorientational motion of molecules along the 3-fold axis relative to the crystallographic [111] direction and also quantifies the orientational disorder within the system. The temperature dependence of $\langle\psi\rangle$ displays three regions:

(i) We define the region up to 400 K as the low-temperature-phase region. In this region, $\langle\psi\rangle$ is less than 10°. This indicates that the molecules exhibit small amplitude reorientational motion. In this region, the increase in $\langle\psi\rangle$ with temperature is significantly smaller.

(ii) The region between 425 and 467 K is defined as the transition region. In this region, $\langle\psi\rangle$ increases considerably with an increase in temperature. A larger value of $\langle\psi\rangle$ indicates that the molecules undergo a large amplitude reorientational motion. This

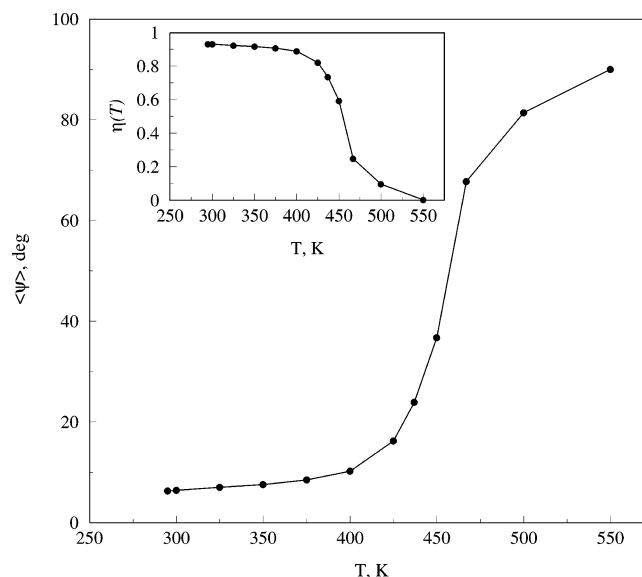


Figure 7. Variation of $\langle\psi\rangle$ as a function of temperature. The inset shows the temperature dependence of the orientational order parameter, $\eta(T)$.

type of broader transition region is common in the simulations of molecular crystals and has been reported in the case of other systems showing orientational⁴⁵ and conformational disorder.⁴⁰

(iii) The region above 467 K is defined as the high-temperature-phase region. In this region, $\langle\psi\rangle$ is closer to 90°. $\langle\psi\rangle$ does not display a significant increase with temperature and eventually it reaches a saturation value of 90°. The saturation value of 90° corresponds to a structure with complete orientational disorder.

Also, we have defined an orientational order parameter, $\eta(T)$ in terms of $\langle\psi\rangle$, to characterize the orientational melting.

$$\eta(T) = \frac{90 - \langle\psi(T)\rangle}{90} \quad (8)$$

The variation of $\eta(T)$ as a function of temperature has been shown in the inset of Figure 7. The variation of $\eta(T)$ as a function of temperature exhibits three different regions as has been observed in adamantane⁴⁴ and poly(tetrafluoroethylene) molecular crystals.⁴⁰ Here, the low-temperature phase is characterized by a value of $\eta(T)$ closer to one and the high-temperature phase is characterized by a value of $\eta(T)$ closer to zero. The value of $\eta(T)$ not equal to one, in the case of the low-temperature phase (i.e., <425 K), is due to the small amplitude librational motion of molecules. The value of $\eta(T)$ equal to zero means a complete orientational disorder and this happens at $T = 550$ K.

Figure 8 shows the variation of compressibility and specific heat as a function of temperature. Compressibility, κ , has been calculated from the volume fluctuation (see eq 9) and specific heat at constant pressure, C_P , has been calculated from enthalpy fluctuation (see eq 10). Both quantities show anomaly at 450 K. As we have described in the earlier section, this anomaly is associated with rotational melting of the orientationally ordered phase resulting in an orientationally disordered phase.

$$\kappa = \frac{\langle V^2 \rangle - \langle V \rangle^2}{\langle V \rangle k_B T} \quad (9)$$

$$C_P = \frac{\langle H^2 \rangle - \langle H \rangle^2}{k_B T^2} \quad (10)$$

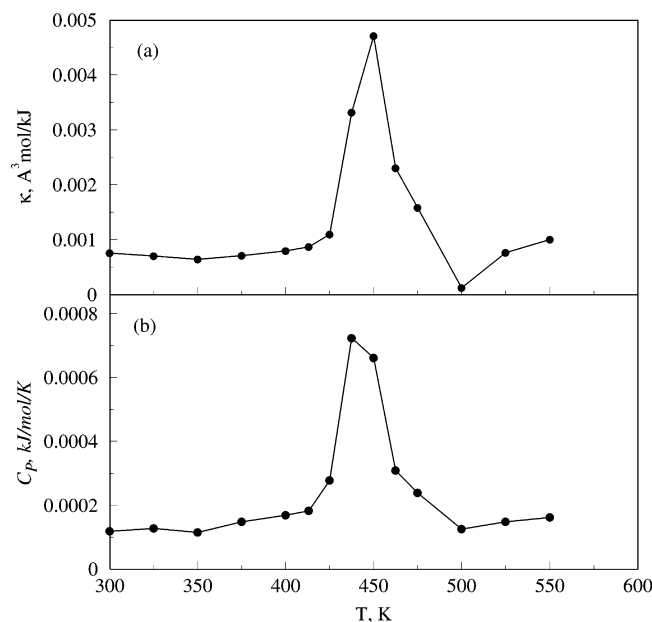


Figure 8. Variation of (a) compressibility, κ , and (b) specific heat at constant pressure, C_p , as a function of temperature.

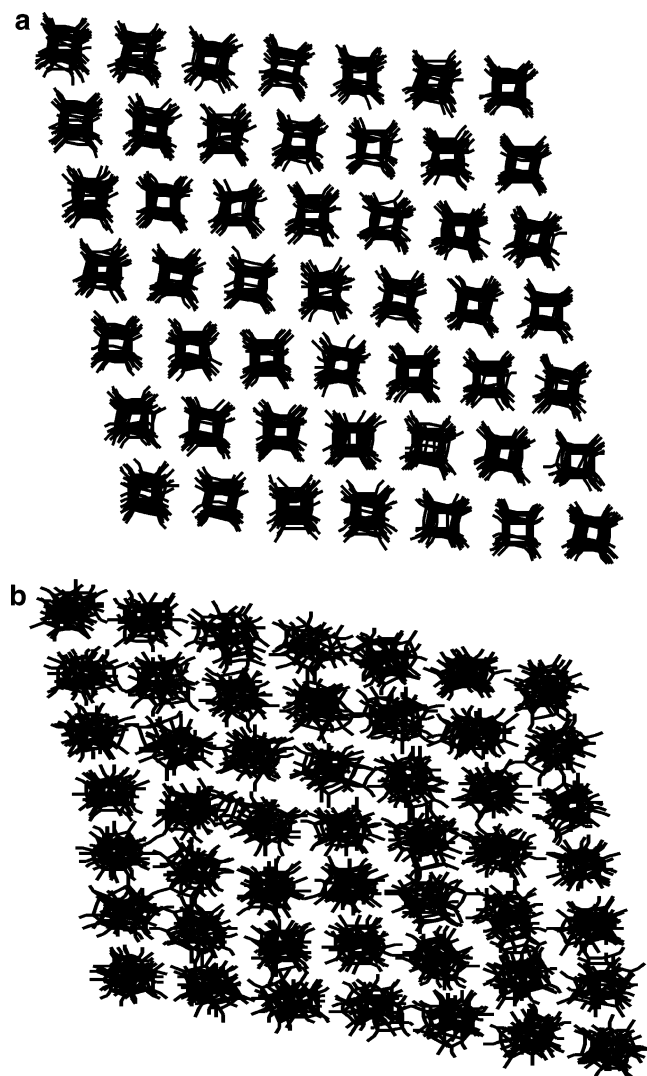


Figure 9. Snapshots along the crystallographic a axis at (a) 300 K, 1 atm, and (b) 500 K, 1 atm.

Here, V is the unit cell volume and H is the enthalpy, which is given by $H = U_{\text{inter}} + PV$.

The enthalpy of transition, ΔH_t , is calculated by integrating specific heat at constant pressure over the temperature range 400–500 K as given in eq 11. The entropy of transition, ΔS_t , is calculated from eq 12. The calculated ΔH_t and ΔS_t are 20.8 J mol⁻¹ and 0.046 J mol⁻¹ K⁻¹, respectively.

$$\Delta H_t = \int_{400}^{500} C_p dT \quad (11)$$

$$\Delta S_t = \int_{400}^{500} \frac{C_p}{T} dT \quad (12)$$

Panels a and b of Figure 9 show snapshots of the cubane molecular crystal at 300 and 500 K and at 1 atm of pressure, respectively. The view is along the crystallographic a axis. It is clearly evident from the figure that at 300 K the cubane molecular crystal has complete orientational order in addition to the translational ordering. Still molecules may exhibit small amplitude rotational as well as translational motion. At 500 K, it is clearly seen from Figure 9b that molecules exhibit many possible orientations relative to each other. At this temperature, the orientational order has disappeared even though translational ordering persists.

4. Conclusions

Orientationally ordered solid cubane shows a transition to an orientationally disordered plastic crystalline phase between 425 and 450 K, which is higher than the experimental transition temperature, 394 K.^{12–15} The transition is characterized to be first order and associated with a 4.8% increase in unit cell volume and a 7% increase in interaction energy. This is in good agreement with the experimentally observed 5.4% increase in unit cell volume.¹⁸ This transition is also associated with discontinuity in second-order quantities such as specific heat at constant pressure and compressibility. The enthalpy (ΔH_t) and entropy (ΔS_t) of transition associated with this transition are 20.8 J mol⁻¹ and 0.046 J mol⁻¹ K⁻¹, respectively. The plastic crystalline phase has a larger thermal expansion than the crystalline phase, which is evident from a larger coefficient of thermal expansion of the plastic crystalline phase when compared to the crystalline phase.

Acknowledgment. The author wishes to thank Prof. S. Yashonath and Dr. A. Sayeed for useful discussions and for providing valuable comments on this manuscript. CMTU, JNCASR is greatly acknowledged for financial support.

References and Notes

- (1) Price, D. L.; Saboungi, M. L.; Bermejo, F. J. *Rep. Prog. Phys.* **2003**, *66*, 407.
- (2) Kolesov, V. P. *Thermochim. Acta* **1995**, *266*, 129.
- (3) Harada, J.; Ogawa, K. *J. Am. Chem. Soc.* **2004**, *126*, 3539.
- (4) Sherwood, J. N. *The Plastically Crystalline State (Orientationally-Disordered Crystals)*; Wiley: New York, 1978; Chapter 1.
- (5) Wasicki, J.; Czarnecki, P.; Katrusiak, A.; Ecolivet, C.; Bertault, M. *J. Phys.: Condens. Matter* **1995**, *7*, 7489.
- (6) Andrew, E. R.; Eades, R. G. *Proc. R. Soc.* **1953**, *A218*, 537.
- (7) Amoureux, J. P.; Bee, M.; Damien, J. C. *Acta Crystallogr. B* **1980**, *36*, 2633.
- (8) Amoureux, J. P.; Sauvajol, J. L.; Bee, M. *Acta Crystallogr. A* **1981**, *37*, 97.
- (9) Dolling, G.; Powell, B. M.; Sears, V. F. *Mol. Phys.* **1979**, *37*, 1859.
- (10) Timmermans, J. *J. Phys. Chem. Solids* **1961**, *18*, 1.
- (11) White, M. A.; Wasylishen, R. E.; Eaton, P. E.; Xiong, Y.; Pramod, K.; Nodari, N. *J. Phys. Chem.* **1992**, *96*, 421.
- (12) Facelli, J. C.; Orendt, A. M.; Solum, M. S.; Depke, G.; Grant, D. M.; Michl, J. *J. Am. Chem. Soc.* **1986**, *108*, 4268.
- (13) Detken, A.; Zimmermann, H.; Haeblerlen, U.; Poupkov, R.; Luz, Z. *J. Phys. Chem.* **1996**, *100*, 9598.

- (14) Dalterio, R. A.; Owens, F. J. *Solid State Commun.* **1988**, *67*, 673.
- (15) Eaton, P. E.; Cole, T. W. *J. Am. Chem. Soc.* **1964**, *86*, 962.
- (16) Yildirim, T.; Ciraci, S.; Kilic, C.; Buldum, A. *Phys. Rev. B* **2000**, *62*, 7625.
- (17) Fleischer, E. B. *J. Am. Chem. Soc.* **1964**, *86*, 3889.
- (18) Yildirim, T.; Gehring, P. M.; Neumann, D. A.; Eaton, P. E.; Emrick, T. *Phys. Rev. Lett.* **1997**, *78*, 4938.
- (19) Yildirim, T.; Gehring, P. M.; Neumann, D. A.; Eaton, P. E.; Emrick, T. *Carbon* **1998**, *36*, 809.
- (20) Yildirim, T.; Gehring, P. M.; Neumann, D. A.; Eaton, P. E.; Emrick, T. *Phys. Rev. B* **1999**, *60*, 314.
- (21) Richardson, S. L.; Martins, J. L. *Phys. Rev. B* **1998**, *58*, 15307.
- (22) Wentzcovitch, R. M.; Martins, J. L.; Price, G. D. *Phys. Rev. Lett.* **1993**, *70*, 3947.
- (23) Yildirim, T.; Kilic, C.; Ciraci, S.; Gehring, P. M.; Neumann, D. A.; Eaton, P. E.; Emrick, T. *Chem. Phys. Lett.* **1999**, *309*, 234.
- (24) Yildirim, T. *Solid State Commun.* **2002**, *124*, 449.
- (25) Kybett, B. D.; Carroll, S.; Natale, P.; Bonnell, D. W.; Margrave, J. L.; Franklin, J. L. *J. Am. Chem. Soc.* **1966**, *88*, 626.
- (26) Pertsin, A. J.; Kitaigorodsky, A. I. *The atom-atom potential method: Applications to organic molecular solids*; Springer series in Chemical Physics; Springer: Berlin, Germany, 1986; Vol. 43.
- (27) Williams, D. E. *J. Mol. Struct.* **1999**, *485-486*, 321.
- (28) Gehring, P. M.; Neumann, D. A.; Kamitakahara, W. A.; Rush, J. J.; Eaton, P. E.; VanMeurs, D. P. *J. Phys. Chem.* **1995**, *99*, 4429.
- (29) Parrinello, M.; Rahman, A. *Phys. Rev. Lett.* **1980**, *45*, 1196.
- (30) Metropolis, N.; Rosenbluth, A. W.; Rosenbluth, M. N.; Teller, A. H.; Teller, E. *J. Chem. Phys.* **1953**, *21*, 1087.
- (31) Yashonath, S.; Rao, C. N. R. *J. Phys. Chem.* **1986**, *90*, 2552.
- (32) Murugan, N. A. Ph.D. thesis, Indian Institute of Science, Bangalore, India, 2004.
- (33) Allen, M. P.; Tildesley, T. J. *Computer Simulation of Liquids*; Clarendon Press: Oxford, UK, 1987.
- (34) Frenkel, D.; Smit, B. *Understanding Molecular Simulations: from algorithms to applications*; Academic Press: San Diego, CA, 1996.
- (35) Yashonath, S.; Rao, C. N. R. *Chem. Phys. Lett.* **1985**, *119*, 22.
- (36) Jin, Z. H.; Gumbsch, P.; Lu, K.; Ma, E. *Phys. Rev. Lett.* **2001**, *87*, 055703.
- (37) Lu, K.; Li, Y. *Phys. Rev. Lett.* **1998**, *80*, 4474.
- (38) Agarwal, P. M.; Rice, B. M.; Thompson, D. L. *J. Chem. Phys.* **1997**, *101*, 2745.
- (39) Velardez, G. F.; Alavi, S.; Thompson, D. L. *J. Chem. Phys.* **2003**, *119*, 6698.
- (40) Sprik, M.; Rothlisberger, U.; Klein, M. L. *J. Phys. Chem. B* **1997**, *101*, 2745.
- (41) Murugan, N. A.; Yashonath, S. *J. Phys. Chem. B* **2005**, *109*, 2014.
- (42) Murugan, N. A.; Yashonath, S. *J. Phys. Chem. B* **2004**, *108*, 17403.
- (43) Murugan, N. A. *J. Chem. Phys.* **2005**, *123*, 094508.
- (44) Depondt, Ph.; Breymann, W. *Mol. Phys.* **1996**, *87*, 1015.
- (45) Ciccotti, G.; Ferrario, M.; Memeo, E.; Meyer, M. *Phys. Rev. Lett.* **1987**, *59*, 2574.